

Electric and Magnetic Fields of the Brain Computed by Way of a Discrete Systems Analytical Approach: Theory and Validation

A. van Rotterdam*

Neurophysiology Group, Department of General Zoology, Biological Centre, University of Amsterdam, Kruislaan 320, NL-1098 SM Amsterdam, The Netherlands

Abstract. It is shown how the stationary volume conduction phenomena in the brain, namely the electric and magnetic fields can be described in discrete terms.

The volume conductor is sampled in space by introducing a sampling distance corresponding to the uncertainty in the measurements. In this way, a three-dimensional lattice is needed with equidistantly spaced nodes. The electric and magnetic properties of such a lattice are assumed to be equivalent to that of brain and other tissues. The electric and magnetic potential fields are calculated for each node as the output of a linear feedback system which has the impressed currents as the input. By way of the feedback loop the reflection phenomena at the boundaries between media of different conductivity can be taken into account.

This discrete formalism has been implemented in a software system. To demonstrate the validity and accuracy of this system a number of analytically tractable problem in volume conduction has been evaluated.

1 Introduction

To analyse electric and magnetic phenomena generated in the nervous tissue, a formulation is used that is based on the volume conduction properties of the excitable tissue. In this way integral expressions for the electric potential and magnetic vector potential field can be derived (Plonsey 1969; Nicholson 1973). These expressions, being surface integrals over rather complicated interfaces, cannot be solved analytically but have to be evaluated by one or another numerical approximation technique. An inevitable question

which arises by using such an approach is what is the accuracy of the approximation with respect to the infinite accuracy of the expression itself; much attention has to be paid to solve this problem (Korn and Korn 1968).

However, one may ask whether this approach is the most useful one. Indeed the implicit assumption is that volume conduction phenomena in the brain can be described in an infinite accurate or continuous way and consequently the discretized expressions, used for numerical computation, should approach the continuous expression as close as possible. Although, to date, complicated volume conduction problems may be tackled by means of the finite element technique implemented on a large computer, one may wonder whether the amount of effort necessary to solve this problem might depend on how the problem was formulated.

On the contrary we choose to reformulate the volume conduction problem in the nervous tissue in discrete terms by defining a priori a measure of uncertainty in location and prescribe that the electric and magnetic potential fields have the form of fields generated in equidistantly spaced resistive and magnetic lattices with an internodal distance or lattice constant equal to the uncertainty measure.

Indeed the continuous description of real physiological systems is often redundant because such systems have intrinsic and inevitable sources of variability and hence can be sufficiently described by specifying them on discrete points in space and time only (Van Rotterdam 1973, 1980).

The behaviour of the lattice fields can be described by means of the formalism proposed here and can be evaluated without considerations concerning the approximation accuracy of the computations if the measure of uncertainty has been chosen in accordance with a priori knowledge about the variability of the physiological system.

* Present address: Radiobiological Institute TNO, Lange Kleiweg 151, NL-2280 HV Rijswijk, The Netherlands

The advantage of the reformulation of volume conduction in discrete terms with respect to the numerical approximation of known integral expressions is that in the former an analytical approach can be followed and a better insight in the properties of the volume conduction in the nervous tissue can be gained. Furthermore it may be hoped that algorithms based on the discrete formalism can be more efficient than the conventional ones.

Finally, it should be noted that the uncertainty distance can be chosen in accordance with the description level of the phenomena. In modelling, e.g., gross electrical behaviour of masses of neurons, as is the case in simulating electro- and magnetoencephalograms, one needs not to describe the details of individual neurons and the uncertainty distance can be taken orders of magnitude larger than the uncertainty distance we have to adopt in modelling extracellular potentials within a certain well defined brain structure such as, for instance, the hippocampus (Habets 1980a, b), the cerebellum (Nicholson and Llinas 1971), the olfactory bulb (Rall and Shepherd 1968) or the olfactory cortex (Freeman 1975).

2 Formalism

2.1 Fundamental Relations

In developing a discrete formalism we start by replacing the volume conductor by a three-dimensional resistive lattice in which the nodes are equidistantly spaced with a lattice constant Δ . The location of a node at $\mathbf{r} = (k\Delta, l\Delta, m\Delta)$ is denoted as (k, l, m) and scalar and vector fields are defined as e.g. $V(k, l, m)$ and $\mathbf{B}(k, l, m) = \{B_x(k, l, m), B_y(k, l, m), B_z(k, l, m)\}$.

Because the sources of electric and magnetic fields in the brain have their main energy in the frequency range below 1 kHz the volume conduction can be considered stationary (Plonsey 1969) and the following relations can be assumed to be valid.

When $J_x(k, l, m)$ is the current in the lattice flowing from node (k, l, m) to node $(k+1, l, m)$, J_y and J_z are defined accordingly, adopting the same convention for the electric field $\mathbf{E}(k, l, m)$ and denoting the conductances at point (k, l, m) by the diagonal matrix

$$g(k, l, m) = \begin{bmatrix} g_x(k, l, m) & 0 & 0 \\ 0 & g_y(k, l, m) & 0 \\ 0 & 0 & g_z(k, l, m) \end{bmatrix} \quad (1)$$

in which $g_x(k, l, m)$ is the conductance between (k, l, m) and $(k+1, l, m)$ etc., we can write a discrete expression denoting Ohm's law:

$$\mathbf{J}(k, l, m) = g(k, l, m)\mathbf{E}(k, l, m) \quad (2)$$

in which $E_x = -\{V(k+1, l, m) - V(k, l, m)\}$ and E_x and E_z are defined accordingly. The dimensions for the quantities are $[\mathbf{J}] = \text{Ampère (A)}$, $[g] = \text{Siemens (S)}$ and $[V] = \text{Volt (V)}$. By defining \mathbf{E} in this way we implicitly introduce a discrete gradient operator \mathbf{D}^+ with the property $-\mathbf{D}^+V = \mathbf{E}$. This is called a forward difference operator because it operates on field values at a node and forwardly located nodes. For the formulation of Kirchhoff's law in the lattice we need a backward discrete divergence operator \mathbf{D}^- which acts on an arbitrary vector field as

$$\begin{aligned} \mathbf{D}^- \cdot \mathbf{A}(k, l, m) = & \{A_x(k, l, m) - A_x(k-1, l, m)\} \\ & + \{A_y(k, l, m) - A_y(k, l-1, m)\} \\ & + \{A_z(k, l, m) - A_z(k, l, m-1)\}. \end{aligned} \quad (3)$$

(Backward difference operators are defined such that they operate on field values at a node and backwardly located nodes.)

The sum of the currents at all nodes being zero is than by means of the discrete divergence operator \mathbf{D}^- expressed as

$$\mathbf{D}^- \cdot \mathbf{J}_t(k, l, m) = 0. \quad (4)$$

When the current field is generated by a so-called impressed current \mathbf{J}_i , the total current \mathbf{J}_t in a lattice consists of that impressed current and the passive part $\mathbf{J} = g\mathbf{E}_0$ obeying Ohm's law, i.e. $\mathbf{J}_t = \mathbf{J}_i + \mathbf{J}$. In case the lattice is homogeneous and isotropic or, in other words, $g(k, l, m) = gI_d$, where I_d is the identity matrix, it follows from (4) that

$$\mathbf{D}^- \cdot \mathbf{E}(k, l, m) = -(1/g)\mathbf{D}^- \cdot \mathbf{J}_t(k, l, m). \quad (5)$$

The assumption that the electric field can be derived from a scalar potential field implies that impressed electromotive forces in the lattice are absent and the potential differences are solely caused by impressed current sources and sinks. Therefore, the sum of potential differences over an arbitrary closed path in the lattice is zero. The conservativeness of the electric field can hence be expressed by means of the discrete curl or rotation operator $\mathbf{D}^+ \times$ as follows:

$$\mathbf{D}^+ \times \mathbf{E}(k, l, m) = \mathbf{0}. \quad (6)$$

It can be easily proved (Van Rotterdam 1986, Chap. II) that just as in conventional vector analysis the following relations for arbitrary fields \mathbf{L} , \mathbf{C} , \mathbf{F} , and \mathbf{M} are equivalent

$$\mathbf{D} \times \mathbf{L}(k, l, m) = \mathbf{0} \quad \text{if and only if}$$

$$\mathbf{L}(k, l, m) = \mathbf{D}\mathbf{C}(k, l, m), \quad (7a)$$

$$\mathbf{D} \cdot \mathbf{F}(k, l, m) = 0 \quad \text{if and only if}$$

$$\mathbf{F}(k, l, m) = \mathbf{D} \times \mathbf{M}(k, l, m). \quad (7b)$$

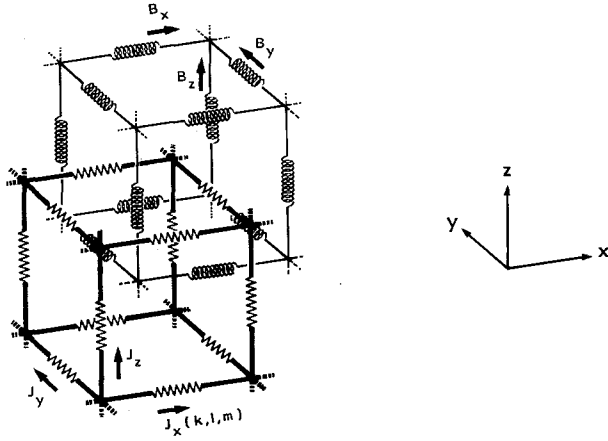


Fig. 1. The resistive and inductive lattice that together represent the discrete medium in which an electric and magnetic induction field can be generated when an impressed current field is defined on the resistive lattice. The nodes of the resistive lattice are connected by resistances whereas the nodes of the inductive lattice are connected by magnetic cores with permeance m_μ .

The operators can be forward or backward difference operators but have to be of the same type in the equivalent relations.

A vector field obeying (7a) is called rotation-free or conservative in discrete sense and can be derived from a scalar potential field while a field obeying (7b) is divergence-free and can be derived from a vector potential field.

For the magnetic phenomena in the lattice one can also set up a set of discrete equations since in every branch of the lattice a current is flowing which necessarily induces a magnetic induction field $\mathbf{B}(k, l, m)$ around that branch.

When we assume, just as for the electric phenomena, that the magnetic induction field can be measured unambiguously only at equidistant points sep-

arated by the lattice distance and when we define the nodal points for the magnetic phenomena (k, l, m) located at $\mathbf{r} = \{(k+0.5)\Delta, (l+0.5)\Delta, (m+0.5)\Delta\}$ as shown in Fig. 1, a discrete formulation of Ampère's induction law is possible.

It will be clear that the assumption of the existence of a discrete magnetic field is equivalent to the assumption that the continuous medium, with a certain magnetic permeability, can be replaced by a three-dimensional lattice in which the nodes are connected by magnetic cores with a certain magnetic permeance, m_μ . In the space outside the lattice the permeability is assumed to be negligible in relation to that in the cores and therefore the magnetic induction outside the lattice can be neglected. It can be proved that in such a magnetic lattice Ampère's law holds and can be described discretely as:

$$\mathbf{D}^- \times \mathbf{B}(k, l, m) = m_\mu \mathbf{J}_t(k, l, m), \quad (8)$$

where the current \mathbf{J}_t is, of course, flowing in the resistive lattice which is separated by a half lattice distance from the magnetic lattice. Analogously to the continuous description, a magnetic field \mathbf{H} is defined as:

$$\mathbf{H}(k, l, m) = (1/m_\mu) \mathbf{B}(k, l, m) \quad (9)$$

while the non-existence of magnetic monopoles is expressed as:

$$\mathbf{D}^+ \cdot \mathbf{B}(k, l, m) = 0. \quad (10)$$

Therefore \mathbf{B} can be derived from a vector potential field \mathbf{A} according to (7b).

It has to be noted that the definition of a vector field in a magnetic lattice is different from the definition in a resistive lattice, i.e. $B_x(k, l, m)$ points to node (k, l, m) from $(k-1, l, m)$ whereas in a resistive lattice a positive vector component points from (k, l, m) to $(k+1, l, m)$.

The properties of the different discrete vector operators are summarized in Table 1.

Table 1

Name	Symbol	Applied on	Results in	Examples
Pos. gradient	\mathbf{D}^+	Scalar field in resistive latt.	Vector field in resistive latt.	$\mathbf{D}^+ V = \mathbf{E}$
Neg. divergence	$\mathbf{D}^- \cdot$	Vector field in resistive latt.	Scalar field in resistive latt.	$\mathbf{D}^- \cdot \mathbf{E} = I/g$
Pos. curl	$\mathbf{D}^+ \times$	Vector field in resistive latt.	Vector field in magnetic latt.	$\mathbf{D}^+ \times \mathbf{E} = 0$
Neg. curl	$\mathbf{D}^- \times$	Vector field in magnetic latt.	Vector field in resistive latt.	$\mathbf{D}^- \times \mathbf{B} = \mathbf{J}$
Pos. divergence	$\mathbf{D}^+ \cdot$	Vector field in magnetic latt.	Scalar field in magnetic latt.	$\mathbf{D}^+ \cdot \mathbf{B} = 0$

2.2 System Equations for the Electric and Magnetic Vector Potential Fields

2.2.1 The Homogeneous Volume Conduction. Taking Eq. (5) and using $\mathbf{E} = -\mathbf{D}^+ V$ one arrives at a second order difference equation for the electric potential field in a homogeneous isotropic lattice, namely:

$$-(\mathbf{D}^- \cdot \mathbf{D}^+) V(k, l, m) = (1/g) I(k, l, m) \quad (11)$$

in which $I(k, l, m) = -\mathbf{D}^- \cdot \mathbf{J}_i(k, l, m)$ is called the current-source density field.

Because this equation is linear the solution field can be written as the following linear combination which is actually a discrete convolution:

$$V(k_0, l_0, m_0) = (1/g) \sum_{k, l, m=-\infty}^{\infty} I(k, l, m) \times G(k_0 - k, l_0 - l, m_0 - m) \quad (12)$$

in which G is a so-called discrete Green's function obeying:

$$-(\mathbf{D}^- \cdot \mathbf{D}^+) G(k, l, m) = \delta_{k0} \delta_{l0} \delta_{m0} \quad (13)$$

in which δ_{k0} is the Kronecker delta $\delta_{k0} = 1$ for $k=0$ and zero elsewhere. In an infinite lattice with the trivial boundary condition that the potential is zero at infinity, G is the potential caused by injection of a unit current at node $(0, 0, 0)$ because for the current field generated by such a point source, $\mathbf{D}^- \cdot \mathbf{J} = 0$ outside $(0, 0, 0)$.

The explicit form of G is difficult to obtain. The only thing that can be said is that for a lattice distance approaching zero G becomes the inverse distance function.

The discrete magnetic vector potential field also obeys a second order difference equation as is derived below. Taking Eq. (8) and using the fact of the divergence-free character of the magnetic induction field $\mathbf{B} = \mathbf{D}^+ \times \mathbf{A}$, it can be proved, just as in the conventional vector analysis, that

$$\begin{aligned} \mathbf{D}^- \times \{\mathbf{D}^+ \times \mathbf{A}(k, l, m)\} \\ = -(\mathbf{D}^- \cdot \mathbf{D}^+) \mathbf{A}(k, l, m) + \mathbf{D}^+ \{\mathbf{D}^- \cdot \mathbf{A}(k, l, m)\} \end{aligned} \quad (14)$$

and it follows that:

$$\begin{aligned} -(\mathbf{D}^- \cdot \mathbf{D}^+) \mathbf{A}(k, l, m) \\ = m_\mu \mathbf{J}_i(k, l, m) - \mathbf{D}^+ \{\mathbf{D}^- \cdot \mathbf{A}(k, l, m)\}. \end{aligned} \quad (15)$$

\mathbf{A} is ambiguously defined because to \mathbf{A} an arbitrary conservative, i.e. rotation-free, component can be added without changing \mathbf{B} . To obtain from (15) an equation in which \mathbf{A} is expressed as a function of impressed currents only we use the ambiguity of \mathbf{A} in such a way that $\mathbf{D}^- \cdot \mathbf{A} = -m_\mu g V$.

Then $\mathbf{D}^+ (\mathbf{D}^- \cdot \mathbf{A}) = m_\mu (\mathbf{J}_i - \mathbf{J}_i)$ so that (15) becomes

$$-(\mathbf{D}^- \cdot \mathbf{D}^+) \mathbf{A}(k, l, m) = m_\mu \mathbf{J}_i(k, l, m). \quad (16)$$

This means that every component of the discrete magnetic vector potential field obeys the discrete equivalent of Poisson's equation as given by expression (11). Therefore, the solution of Eq. (16) in an infinite homogeneous lattice is given by the following convolution

$$\begin{aligned} \mathbf{A}(k_0, l_0, m_0) = m_\mu \sum_{k, l, m=-\infty}^{\infty} \sum_{k, l, m=-\infty}^{\infty} \mathbf{J}_i(k, l, m) \\ \times G(k_0 - k, l_0 - l, m_0 - m). \end{aligned} \quad (17)$$

Indeed by comparing (17) with (12), it follows that $\mathbf{D}^- \cdot \mathbf{A} = -m_\mu g V$ as was defined above.

To obtain the magnetic and electric potential field in a homogenous lattice caused by a certain impressed current field it therefore suffices to evaluate the magnetic vector potential field and to derive the electric potential field from it by a simple divergence operation. However, the magnetic induction field cannot be derived from the electric field because the magnetic phenomena depend on the rotational aspects of the impressed current field which do not play a role in the behaviour of the electric potential field. The latter depends only on the amount and location of the current injected in and extracted from the medium and not on the direction of the impressed currents.

2.2.2 The Inhomogeneous Volume Conductor. Expressions (12) and (17) described the electric and magnetic fields in a homogeneous and infinite medium. However the brain tissue is far from homogeneous and, evidently, not infinite so that the above expressions cannot be used directly to simulate in a realistic way the electric and magnetic phenomena of the brain. In this section we therefore extend the formalism in such a way that it will be possible to deal with inhomogeneities.

Furthermore at the macroscopic level when one is interested in analysing electro or magnetoencephalographic phenomena, one has to consider the different tissues, which surround the brain and have conductivity properties different from gray and white matter, namely the scalp, the skull and the cerebrospinal fluid (CSF). At the microscopic level of a given structure within the brain one has to distinguish differences in the density of neuronal populations and fibre systems. At this microscopic level the neuronal structures can be considered to behave as bodies with a constant conductivity immersed in a conductive medium having also a constant but different conductivity. At an even finer scale namely the ultra-microscopic level one must distinguish a complex organization of extracellular space and sub-cellular processes; for example the extracellular space appears to be composed of a complicated mesh that has been called the "extracellular jungle" (Nicholson 1980). At this level the medium can no longer be considered piece-wise homo-

geneous and isotropic and the stationarity assumption does not hold because the microscopic ion concentrations change in time in a non-stationary way.

For modelling electro- and magnetoencephalograms (EEGs and MEGs) measured at the scalp, a global or macroscopic level of description is sufficient. For modelling phenomena as encountered in electrophysiological measurements within the brain, for instance extracellular field potentials in vivo or in vitro preparations, the microscopic level of description is necessary.

The separate neurons are considered to behave as generators of extracellular currents owing to membrane processes which in their turn are dependent on synaptic actions. The ultra-microscopic level of description falls outside the scope of the study and will not be discussed here.

2.2.3 Linear Systems Analysis of Inhomogeneous Volume Conduction. To obtain insight in the function of the various difference operators which are involved in non-homogeneous volume conduction, we adopt the so-called linear systems analysis approach. It is well known that in the analysis of linear time-invariant systems as used in communication theory (Cheng 1961) this technique offers the advantage of simplicity in the description of systems properties.

According to this approach the electric and magnetic fields can be considered as the outputs of a linear system representing the volume conduction properties. The system is described by a combination of difference and multiplication operators. The input of the system is the impressed current field. As will be shown below non-homogeneous properties of the volume conductor can be accounted for by the introduction of a feedback loop representing phenomena at the boundaries of changing conductivity.

To arrive at a system equation for the electric potential field in a non-homogeneous isotropic lattice we start from the equation

$$-\mathbf{D}^- \cdot \{g(k, l, m)\mathbf{D}^+ V(k, l, m)\} = I(k, l, m) \quad (18)$$

which follows directly from the definition of \mathbf{E} and the divergence-free character of the sum of impressed and passive currents. Contrary to the homogeneous case the conduction tensor can no longer be replaced by a constant but has to be represented by the scalar function $g(k, l, m)$.

In Eq. (18) the product of the scalar field g and the discrete gradient $\mathbf{D}^+ V$ can be rewritten by means of the product divergence rule as follows:

$$\begin{aligned} g(k, l, m)\mathbf{D}^+ V(k, l, m) &= \mathbf{D}^+ \{g(k, l, m)V(k, l, m)\} \\ &\quad - \{\mathbf{D}^+ g(k, l, m)\} V(k, l, m) \\ &\quad - \{\mathbf{D}^+ g(k, l, m)\} \otimes \{\mathbf{D}^- V(k, l, m)\} \end{aligned} \quad (19)$$

in which the direct vector product denoted by $\mathbf{A} \otimes \mathbf{B}$ is defined as $\mathbf{A} \otimes \mathbf{B} = (A_x B_x, A_y B_y, A_z B_z)$.

Substitution of (19) into (18) results in the following system equation for the potential field V caused by the impressed current field \mathbf{J}_i .

$$\begin{aligned} [-\mathbf{D}^- \cdot \mathbf{D}^+] [g(k, l, m)] V(k, l, m) &= -[\mathbf{D}^- \cdot] \{\mathbf{J}_i(k, l, m) \\ &\quad + \mathbf{D}^+ g(k, l, m)\} V(k, l, m) \\ &\quad + [\mathbf{F}_i(k, l, m)] V(k, l, m) \end{aligned} \quad (20)$$

in which the square brackets are used to denote the separate linear difference and multiplication operators involved in the non-homogeneous volume conduction.

Furthermore, in expression (20) the direct vector product operator $\mathbf{D}^+ g \otimes \mathbf{D}^-$ acting on V has been written as a rest operator \mathbf{F}_i , the effect of which can be discarded in relation to the other operators in case the lattice distance Δ approaches zero because it contains an extra difference operator.

Until here we have not taken into consideration the magnetic phenomena in a magnetically homogeneous but electrically nonhomogeneous medium. As said before, the magnetic field is determined by the rotational components of the impressed current field while the electric field is only determined by what results of the impressed current field after a divergence operation. However, both fields are interdependent. Actually, once the magnetic vector potential has been found, the electric potential field can be obtained by a simple difference operation from the magnetic vector potential field. Therefore we should consider both phenomena as originating from one system with the impressed current field \mathbf{J}_i as input.

Because the magnetic induction \mathbf{B} is only dependent on the rotational aspects of the current field, the passive current field $g\mathbf{E}$, being conservative in the homogeneous lattice, has no influence on the magnetic induction field in such a volume conductor. However, in a non-homogeneous lattice, the passive current field is not necessarily completely rotation-free, but can have rotational components at the boundaries between media with different conductances.

The system operation for the magnetic vector potential \mathbf{A} in the non-homogeneous lattice can be derived from Eq. (15), defining, just as in the homogeneous case, $\mathbf{D}^- \cdot \mathbf{A} = -m_\mu g(k, l, m)V(k, l, m)$ and using (19) it follows that

$$\begin{aligned} [-\mathbf{D}^- \cdot \mathbf{D}^+] \mathbf{A}(k, l, m) &= m_\mu \{\mathbf{J}_i(k, l, m) \\ &\quad + [\mathbf{D}^+ g(k, l, m)] V(k, l, m) \\ &\quad + [\mathbf{F}_i(k, l, m)] V(k, l, m)\} \end{aligned} \quad (21)$$

Equations (20) and (21) prescribe the behaviour of the electric (V) and magnetic vector potential (\mathbf{A}) field in a magnetically homogeneous but for conductance non-

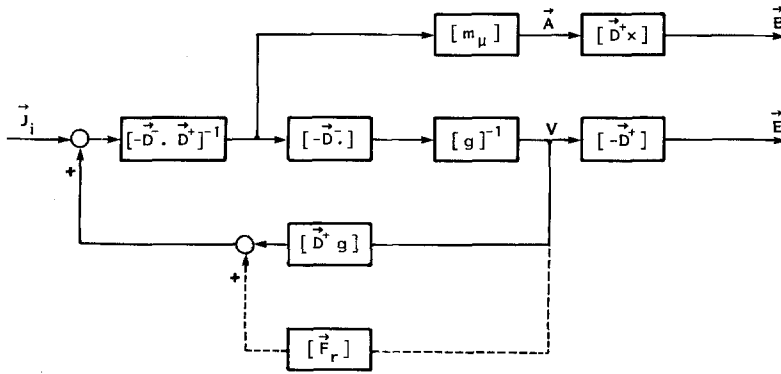


Fig. 2. Block diagram of the complete discrete volume conduction system for both magnetic and electric fields. The rest system in the feedback loop is connected by dashed lines to denote that eventually this subsystem can be left out without changing the overall system behaviour too much

homogeneous lattice excited by an impressed current field \mathbf{J}_i .

The volume conductor system can be symbolically depicted by the block diagram of Fig. 2. It can be immediately seen from this diagram that the electric potential field can be derived from the magnetic vector potential field and the inhomogeneities in the conductance cause reflection phenomena at the boundaries between media with different conductances which influence not only the electric but also the magnetic field.

3 Algorithm and Simulation System

In order to compute magnetic induction and electric potential fields caused by a certain impressed current configuration in a non-homogeneous volume conductor with a certain conductivity structure, the system of Fig. 2 has been implemented on a minicomputer (PDP 11/34). This simulation system is based on an algorithm which is discussed below.

As can be seen from expressions (20) and (21) the outputs will be sums of discrete Green's functions because V , E , and B are generated by a linear feedback system in which the discrete inverse Poisson's or homogeneous volume conduction operator $[-\mathbf{D}^- \cdot \mathbf{D}^+]^{-1}$ plays a major role. The discrete Green's function (i.e. the potential field response to a unit current injection in an infinite lattice) has, in theory, an infinite extent. However, assuming that the volume conductor is discrete implies that field variations within the lattice distance have no meaning and hence field amplitudes have also a certain indeterminacy.

Therefore the infinite Green's function is not distinguishable from the approximated function with a finite extent. This can be realized by constructing a periodical Green's function and taking the primary part.

In this way we can carry out the simulations of electric and magnetic fields in the nervous tissue using periodic discrete configurations. It is, of course, im-

portant to choose a spatial period large enough, such that the aliasing effects do not cause deviations in amplitude which exceed the variance of experimental values.

The best way to analyse discrete periodic systems is to use the discrete Fourier transformation (DFT). This implies that the various system operators must be written in the spatial frequency domain. In the homogeneous case the system consists solely of difference operators, namely $[\mathbf{D}^- \cdot]$, $[\mathbf{D}^+ \times]$, and $[-\mathbf{D}^- \cdot \mathbf{D}^+]^{-1}$ which take a very simple form in the spatial frequency domain, namely these become multiplication operators.

In the inhomogeneous case, however, the multiplication operators in the spatial domain $[\mathbf{D}^+ g]$, $[\mathbf{F}_r]$, and $[g]^{-1}$ play a role which is location dependent and therefore they transform to convolution operators in the spatial frequency domain.

However, the complete inhomogeneous volume conduction operation depicted in Fig. 2 cannot be put in multiplicative form neither in the spatial nor in the spatial frequency domain. To solve this problem we followed an iterative approach in which in every step of the iteration the fields are transformed from the spatial to the spatial frequency domain in which the difference operations are performed. Then an inverse transform is applied and the influence of the feedback loop is computed in spatial domain, and the process is repeated iteratively.

Because, as can be seen from Fig. 2, the electric potential field V is the only quantity that influences the feedback term, the iterative scheme has only to be applied to approximate V . Once a satisfactory approximation to the electric potential field has been found, V can be used to compute the boundary currents $[\mathbf{D}^+ g] V$ which together with the impressed current field \mathbf{J}_i generate the magnetic induction field \mathbf{B} .

There are several ways to compute iteratively the response of a nonhomogeneous feedback system to a given input. The best one has to be selected using the criterion of convergence speed, i.e. to reduce to a minimum the number of iteration steps that are needed

to reach a satisfactory approximation. It has been shown (Van Rotterdam 1986, Chap. VI) that a conventional iteration, in which in every step \mathbf{D}^+g is to be computed, functions in a highly location dependent fashion, i.e. at some locations a satisfactory approximation can be obtained after a few iteration steps, whereas at other locations one needs many more steps to achieve the same accuracy.

Therefore, we adopted the Wittmeyer scheme (Stoer and Bulirsch 1973) by which it is possible to locally influence the convergence speed of the iteration procedure. Without going into detail here (cf. Van Rotterdam 1986, Chap. IV) we can mention that the multiplicative effect of the conductance, expressed by the operator $[g]^{-1}$ in Fig. 2, is evaluated partly recursively and partly directly. To that end g is considered to consist of two factors, namely g_A which acts locally and the effect of which is computed directly and a second factor g_B , the effect of which is evaluated iteratively in the same iteration procedure which is used for the evaluation of the feedback contribution.

The software system used to implement this makes use of the fast Fourier transform (FFT) algorithm as described by Singleton (1967). This algorithm has been developed to compute the FFT with auxiliary memory and is suited for the transformation of large amounts of data on relatively small computer systems with additional disks for mass storage of data as described in Van Rotterdam (1986, Chaps. V and VII).

4 Results

In order to demonstrate the applicability of the discrete formalism and the developed algorithm we consider some analytically tractable electric and magnetic fields in a homogeneous volume conductor generated by *a*) an elementary impressed current vector; *b*) a coil shaped impressed current and *c*) an elementary closed surface on which a constant impressed current was defined.

All simulations were computed with scaled conductances and arbitrary impressed current strengths. In the homogeneous computations a conductance of 1S over one lattice distance was chosen (thus simulating a medium with a conductivity of 2×10^4 S/m when $\Delta = 50 \mu\text{m}$). When the unit current is chosen 1A in such a lattice 1 unit of electric potential (u.e.p.) is equivalent to 1V.

i) In Fig. 3 the electric and magnetic field characteristics caused by an elementary impressed current vector in the x -direction $\mathbf{J}_i = \mathbf{n}_x \delta(k - k_0, l - l_0, m - m_0)$ located at node $(k_0, l_0, m_0) = (16, 16, 4)$ in an $32 \times 32 \times 8$ dimensional lattice are shown. Figure 3a, b, and c depict the characteristics of the electric potential field

generated by the negative divergence of \mathbf{J}_i forming a sink-source pair at the above given location.

A qualitative impression of the magnetic induction field \mathbf{B} caused by the elementary impressed current can be obtained from Fig. 3d which shows the vector map of \mathbf{B} in the $y-z$ plane through $x=16$. B_x is absent which is in accordance with the theory which says that the magnetic field, being the rotation of the vector potential field \mathbf{A} which is in the direction of \mathbf{J}_i , is perpendicular to that vector. Both the y and z components of \mathbf{B} have a maximum of 0.1666 units of magnetic induction (u.m.i.) and together form a vector field which rotates counter-clockwise. This means that the current vector is pointing towards the observer, i.e. in the x -direction.

ii) In Fig. 4, various aspects of the behaviour of an induction field generated by three closed square-shaped impressed current loops, in a $8 \times 8 \times 8$ lattice simulating a coil with three windings, is shown. Because the impressed current field in such a "coil" is divergence-free no electric potential was generated. Figure 4a-c show the behaviour of the separate components of \mathbf{B} in the $x-y$ plane at $z=4$ through the axis of the "coil".

To represent the behaviour of \mathbf{B} in a way which is easy to interpret we also constructed a vector density plot in Fig. 4d. Vector density lines are constructed in such a way that the strength of the vector field corresponds to the number of lines per surface unit and the direction of the field to the direction of the lines.

Formally, these lines can only be drawn in a certain plane when the vector field is derived from a vector potential field which is perpendicular to that plane. Although for the induction field of the "coil" such planes do not exist we nevertheless can obtain a qualitative impression of the strength and orientation of the induction field by integrating the $B_{x,y}$ components at $z=4$ to obtain the part of \mathbf{A} which is perpendicular to the $x-y$ plane. In this way isovalue lines of that part \mathbf{A} can be constructed.

To evaluate the influence of the limited size of the lattice another simulation was performed in a lattice of dimensions $64 \times 64 \times 8$ with the same "coil" as mentioned above. Figure 4e shows vector density lines in this large lattice at $z=4$. Owing to the large dynamic range of the lattice the density lines are smoother than these in Fig. 4d. However, the same features of the field are shown in both simulations.

iii) A critical test to evaluate the performance of the simulation system consists in computing the fields of a constant impressed current configuration on the smallest possible closed surface, i.e. a square box containing only one lattice point. The electric potential field for such a configuration ought to be constant inside the

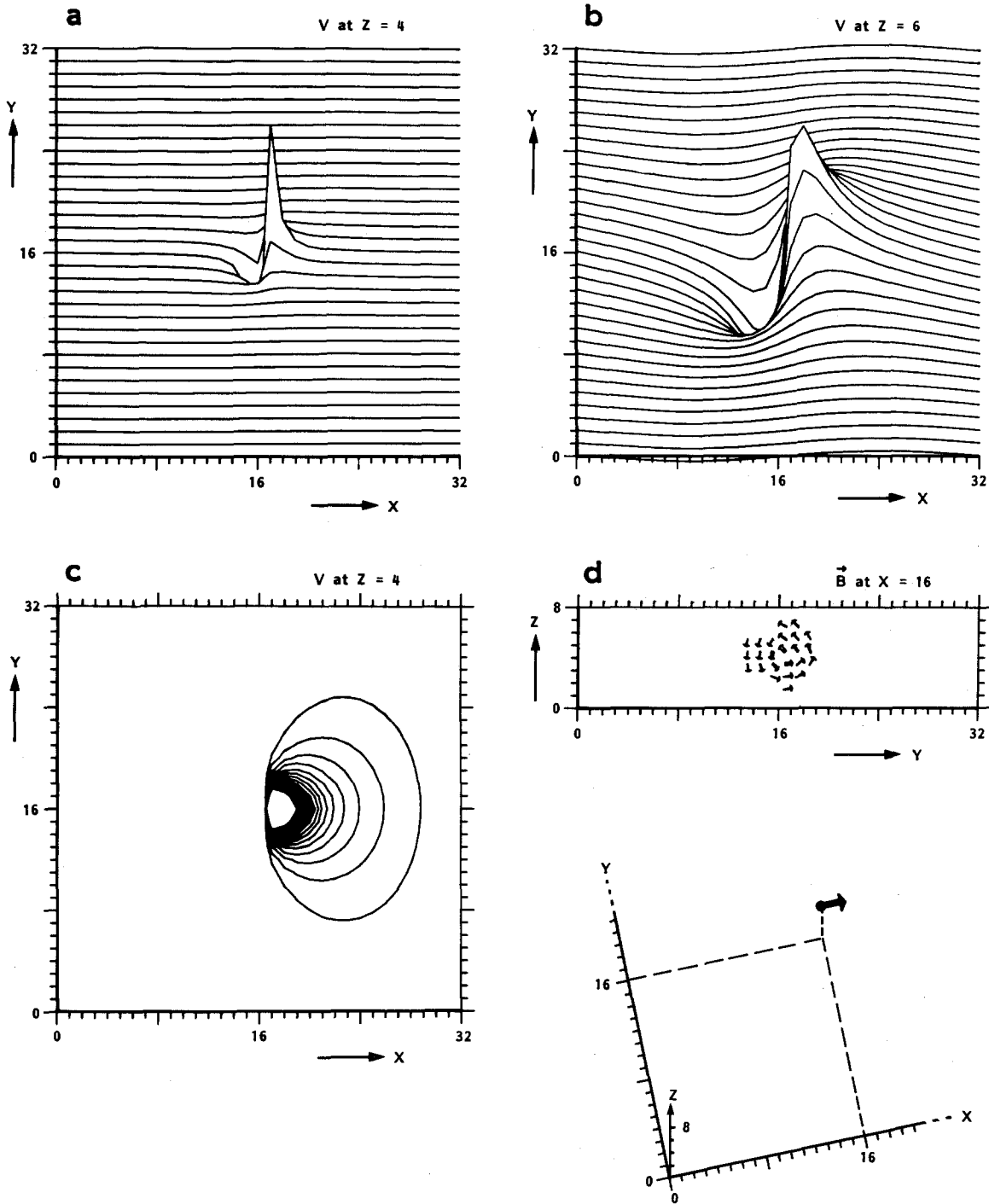


Fig. 3a-d. Inset: (right below) location of the impressed current vector, \mathbf{J}_i at node $(k_0, l_0, m_0 = 16, 16, 4)$ which points in the x-direction. **a** Amplitude plot of the electric potential field at $z=4$ generated by a single impressed current vector \mathbf{J}_i . The potential field as function of the x - and y -coordinates is a dipole field caused by the sink source character of the discrete gradient of the impressed current vector. The maximum amplitude corresponds to a potential of 0.1666 units of electric potential (u.e.p.). **b** The same potential field but now plotted in the x - y plane at $z=6$ (n.b.: the amplitude plots are drawn in full scale, so-called hidden lines are not drawn which means that the line segments in the plot which graphically are behind other lines are not shown). **c** Positive contour lines of the potential function shown in a. 21 isopotential lines are drawn between the value of 0.0167 and 0 u.e.p. as follows: the outer line is at potential $(1/22) \times 0.0167$ u.e.p. and the inner line at $(21/22) \times 0.0167$ u.e.p. The negative contour lines have been omitted. **d** Vector map of the magnetic induction field generated by the single impressed current vector measured in the y - z plane at $x=16$. The width of the vector is a measure of the strength of the field, i.e. the modulus of the vector field. Only magnetic induction components within the bounds of 0.4711 and 0 units of magnetic induction (u.m.i.) are drawn

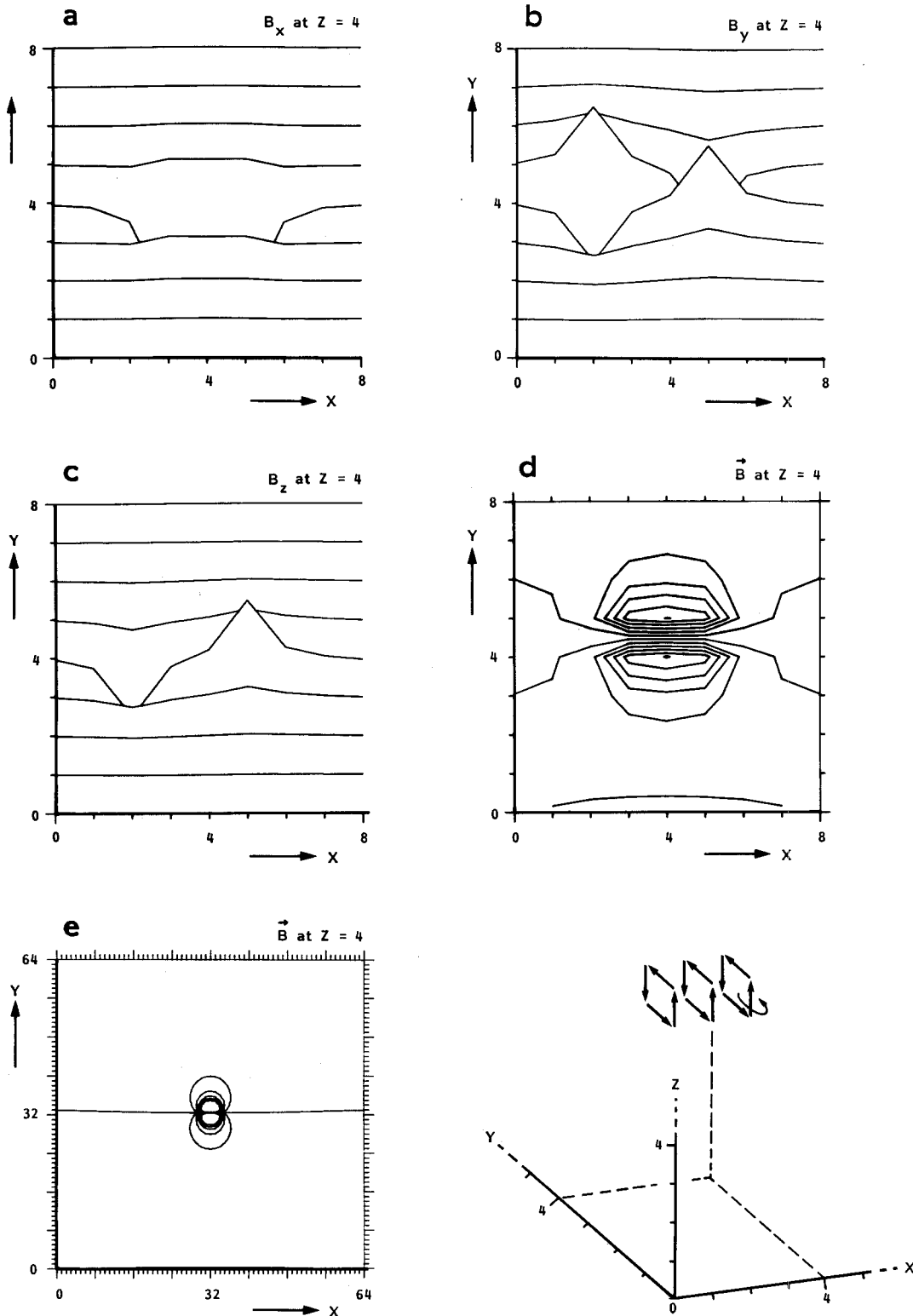


Fig. 4a-e. Magnetic induction field of a coil-shaped impressed current configuration. Inset: The location of the input current configuration in an $8 \times 8 \times 8$ dimensional lattice. **a** Amplitude plot of the x-component of \vec{B} in the $x-y$ plane at $z=4$. Maximum $= 0.0448$ and minimum $= -0.9100$ u.m.i. **b** The y-component of \vec{B} in the sample plane. Maximum $= 0.1644$ and minimum $= -0.1644$ u.m.i. **c** The z-component of \vec{B} in the sample plane. Maximum $= 0.1644$ and minimum $= -0.1644$ u.m.i. **d** Vector density lines in the $x-y$ plane at $z=4$. **e** The same but now for the coil configuration located at $(32, 32, 4)$ in a $64 \times 64 \times 8$ dimensional lattice. Owing to the small size of the coil in relation to the size of the lattice the magnetic field has a limited extent in this plot

box and zero outside. On the other hand the constant impressed current configuration is conservative and hence the magnetic induction field ought to be zero everywhere in the lattice.

In simulating the fields in a $4 \times 32 \times 4$ dimensional lattice no induction was found whereas the electric potential field was an impulse function of -1 u.e.p. inside the box superimposed on a constant field of $1/n_x \cdot n_y \cdot n_z$ u.e.p. These numerical results are completely in accordance with the theory when we take into account that the software system filters out the zero spatial frequency component. Therefore the sum of all potential values over the lattice (being the zero spatial frequency component) should be zero. This is the reason why the simulated potential field is superimposed on a constant positive field which together with the field inside the box sums up to zero.

5 Discussion

The purpose of the work reported here was to develop a general formalism for the description of electric as well as magnetic volume conduction phenomena of various kinds in the brain; to develop algorithms based on this formalism and to construct computer programs by means of which problems encountered in electro- and magnetoencephalography and in experimental electrophysiology may be simulated. It is convenient to inquire whether the method developed here satisfies the three general criteria (Viergever 1980) for a good model, namely *a*) simplicity in description, *b*) interpretability of results and *c*) agreement of model results with available experimental data.

a) The model is simple because the discrete formalism avoids the description of useless details which only complicate the numerical evaluation of fields. This is possible by virtue of the fact that bioelectric and biomagnetic phenomena are intrinsically of a stochastic character and hence can be represented as discrete signals defined on resistive and magnetic lattices with a constant internodal distance. In this sense this approach has to be distinguished from the finite element method, by which it is possible to evaluate numerically integral or differential expressions by means of non-equidistantly spaced lattices.

b) The second criterion to be satisfied is that the model gives good insight into the problem. Stationary volume conduction has already been described in the 19th century and Green's identities (Jackson 1962) have been used to formulate many problems with various degrees of complexity. However, the real physical meaning of phenomena described by vector analytical expressions appears to be not easily acceptable.

In contrast, the simulations which can be made using the algorithm introduced here, can be directly interpreted in simple biophysical terms.

c) The third criterion to be satisfied is that the simulation results are in good agreement with experimental data. It has to be kept in mind here that in brain research experimental data are necessarily incomplete, i.e. it is impossible in general to measure fields in the whole volume conductor. This is especially the case in electroneurological practice where EEG potentials are measured at the scalp, at most 21 locations, whereas MEG fields can, at present, be measured only at a few locations. The inverse problem can therefore not be solved in a unique way (Cuppen 1983).

Of course, taking into consideration the limitations imposed by experimental measurements in brain research it will be clear that an agreement between model and experimental data can only be judged in a qualitative sense. We therefore consider a simulation to be satisfactory when the same general properties of the experimental measurements may be represented by the biophysical model which is simulated using the approach presented here.

References

- Cheng DK (1961) Analysis of linear systems. Addison Wesley, Reading, Mass
- Cuppen JJM (1983) A numerical solution of the inverse problem of electrocardiography. Thesis, University of Amsterdam, The Netherlands
- Freeman W (1975) Mass action in the nervous system. Academic Press, New York
- Habets AMMC (1980a) The projection of the prepyriform cortex to the hippocampus in the cat. Thesis, State University of Utrecht, The Netherlands
- Habets AMMC, Lopes da Silva FH, Mollevanger WJ (1980b) An olfactory input to the hippocampus of the cat: field potential analysis. *Brain Res* 182:47-64
- Jackson JD (1962) Classical electrodynamics. Wiley, New York
- Korn GA, Korn TM (1968) Mathematical handbook for scientists and engineers. McGraw-Hill, New York
- Nicholson C (1973) Theoretical analysis of field potentials in anisotropic ensembles of neuronal elements. *IEEE Trans BME* 20:278-288
- Nicholson C (1980) Dynamics of the brain cell environment. *Neurosci Res Prog Bull* 18:177-322
- Nicholson C, Llinas R (1971) Field potentials in the alligator cerebellum and theory of their relationships to Purkinje cell dendritic spikes. *J Neurophysiol* 34:509-531
- Plonsey R (1969) Bioelectric phenomena. McGraw-Hill, New York
- Rall W, Shepherd GM (1968) Theoretical reconstruction of field potentials and dendro dendritic synaptic interaction in olfactory bulb. *J Neurophysiol* 31:884-915

- Reite H, Zimmerman JE, Edrich J, Zimmerman J (1976) The human magnetoencephalogram: some EEG and related correlations. *Electroenceph Clin Neurophysiol* 40:59–66
- Rotterdam A van (1973) A discrete formalism for the computation of extracellular potentials. *Kybernetik* 12:223–228
- Rotterdam A van (1980) A computer system for the analysis and synthesis of field potentials. *Biol Cybern* 37:33–39
- Rotterdam A van (1986) Electric and magnetic fields of the brain; a systems analytical approach. Thesis, University of Amsterdam, The Netherlands
- Singleton RC (1967) A method for computing the fast Fourier transform with auxiliary memory and limited high speed storage. *IEEE Trans AEA-15*:91–98
- Stoer J, Bulirsch R (1973) Einführung in die numerische Mathematik, II. Springer, Berlin Heidelberg New York
- Viergever MA (1980) Mechanics of the inner ear. Thesis, Delft University of Technology, The Netherlands

Received: March 13, 1987

Dr. A. van Rotterdam
TNO Radiobiological Institute
P.O. Box 5815
Lange Kleiweg 151
NL-2280 HV Rijswijk
The Netherlands